Chinese Chemical Letters 33 (2022) 683–692

Contents lists available at ScienceDirect

Chinese Chemical Letters

journal homepage: www.elsevier.com/locate/cclet

Bifunctional carbon-based cathode catalysts for zinc-air battery: A review

Huimin Liu[a], Qinglei Liu[a], Yarong Wang[a], Yongfei Wang[a,b,*], Shulei Chou[c,*], Zhizhi Hu[a], Zhiqiang Zhang[a,*]

[a] Key Laboratory for Functional Material School of Chemical Engineering, University of Science and Technology Liaoning, Anshan 114051, China
[b] School of Materials and Metallurgy, University of Science and Technology Liaoning, Anshan 114051, China
[c] Institute for Carbon Neutralization, College of Chemistry and Materials Engineering,Wenzhou University, Wenzhou 325035, China

ARTICLE INFO

Article history:
Received 9 June 2021
Revised 12 July 2021
Accepted 13 July 2021
Available online 20 July 2021

Keywords:
Carbon materials
Defect
Doping, Oxygen evolution reaction
Oxygen reduction reaction
Zinc-air battery

ABSTRACT

Efficient bifunctional OER/ORR catalysts are crucial for the further development of zinc-air battery. From a sustainable point of view, it is important that electrocatalysts are efficient, low cost, and composed of abundant resources instead of scarce metals. Due to their good conductivity, low cost, and strong durability, carbon-based materials are considered a promising alternative in the field of commercial zinc-air battery catalysts. Herein, we briefly introduce the zinc-air battery and then summarize recent progress in the development of carbon-based bifunctional catalysts by defect engineering, heteroatom doping and metal doping. Finally, we discuss the main challenges and prospects for the future development of carbon-based bifunctional oxygen catalysts.

1. Introduction

Due to the economic, scientific, and technological development over the past several decades, human society has made significant progress in many areas such as the chemical industry, environmental protection, medical treatment, electronics, and energy production. However, the consumption of nonrenewable energy has increased with global economic development. The emergence of clean solar and wind energy can solve many of the issues caused by this energy crisis. However, renewable energy output is greatly affected by season, climate, and location, and cannot be controlled as needed. Therefore, in order to effectively utilize solar energy and wind energy, the development of low-cost, sustainable, and highly efficient energy conversion and storage technologies is of utmost importance [1–4]. Due to their high energy density, low cost, wide range of use, safety and reliability, zinc-air battery have broad commercialization prospects [5,6].

The oxygen evolution reaction (OER) and oxygen reduction reaction (ORR) are the basis for converting chemical energy into electrical energy. These reaction processes are complex and their kinetics is slow. Furthermore, their practical energy efficiency and cycle stability are far from satisfactory [7,8]. Although Zn and O_2 can react spontaneously, the kinetics of ORR are slow in the process of battery discharge, requiring the participation of a catalyst to accelerate the reaction. Meanwhile, effective OER catalysts are also essential to realize rechargeable zinc-air battery. Currently, the best ORR catalyst is Pt, but the activity of Pt for OER is not satisfactory. RuO_2 and IrO_2 are the benchmark OER catalysts, but they have poor ORR performance. Although a combination of these two catalysts can achieve bifunctional catalysis, this results in a complex process and high price [9–11]. Therefore, the design of efficient, stable, and low-cost bifunctional catalysts for both ORR and OER is urgently required.

Recently, carbon-based materials, transition metal-based materials and their derivatives (oxides/sulfides/hydroxides), and composites have been extensively explored as alternative materials for bifunctional catalysts. Although transition metal-based catalysts have good redox electrochemical properties, their poor conductivity and dispersion limits their application. Carbon-based materials have various structures such as 0D (*e.g.*, fullerene), 1D (*e.g.*, carbon nanotubes (CNTs)), 2D (*e.g.*, graphene) and 3D (porous carbon nanostructures) morphologies. These morphologies provide more exposed active sites and result in faster mass transfer. Moreover, due to their high conductivity, high specific surface area, good corrosion resistance, and low cost, carbon-based materials have aroused a significant amount of research interest [12–16]. The free electrons in sp^2 carbon structures can ensure rapid charge transfer in redox reactions. In addition, their electronic structure can

* Corresponding authors.
E-mail addresses: wyf8307@ustl.edu.cn (Y. Wang), chou@wzu.edu.cn (S. Chou), zzq@ustl.edu.cn (Z. Zhang).

https://doi.org/10.1016/j.cclet.2021.07.038
1001-8417/

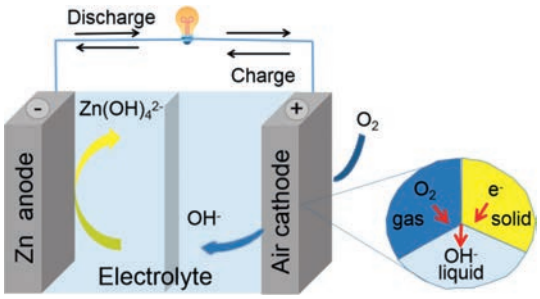

Fig. 1. Basic Zn-air battery configuration and simplified solid-liquid-gas three-phase interaction.

be easily adjusted by heteroatom doping, defect engineering, or in combination with other metals to improve catalytic performance. Although several reviews have summarized carbon-based materials as bifunctional electrocatalysts in zinc-air battery, it is necessary to provide an updated summary of the large amount of recent research in this area.

Therefore, in this review, we first summarize the working principles of zinc-air battery and the related reaction mechanism of oxygen reactions. Subsequently, emerging carbon-based bifunctional electrocatalysts are presented, paying particular attention to changes to catalyst size and structure as well as new strategies for improving catalyst performance. These electrocatalysts are synthesized by defect engineering, heteroatom doping and metal doping. Finally, we describe the current challenges and future perspectives of carbon-based bifunctional oxygen catalysts for meeting the performance requirements of zinc-air battery. We expect that this review will provide timely information for future research and identify directions for the future development of electrocatalysts with high activity, a long life, and good performance in zinc-air battery.

2. Electrically rechargeable zinc-air battery

Zinc-air battery is a type of metal-air battery. This technology is relatively mature and was initially developed in the 19th century. In 1878, Maiche *et al.* used a porous carbon electrode containing platinum as a positive electrode to assemble the earliest zinc-air battery. The electrode performance of this battery was very poor because a slightly acidic electrolyte was used [17]. In 1932, Heise and Schumacher used an alkaline electrolyte to prepare a zinc-air battery, significantly increasing the discharge current. However, output power was low [18]. Since then, many countries around the world have developed and promoted zinc-air battery. Today, they are widely used in communication base stations, electric bicycles, seismic telemetry, energy storage, and electric vehicles [19–21]. They have the advantages of high energy density, a stable electrolyte and low cost [22,23].

2.1. Battery configuration

Zinc-air battery use metal zinc as the anode, oxygen in the air or pure oxygen as the cathode, and are encapsulated with an electrolyte, as shown in Fig. 1. Zinc electrodes are usually made of zinc powder, a zinc plate, or zinc foam. The most commonly used electrolytes in zinc-air battery are alkaline solutions such as KOH, NaOH and LiOH. Among these, KOH solution has been widely used because of its good conductivity, high mass transfer rate, and high zinc salt solubility [24–29]. Generally, a small quantity of $ZnCl_2$ (*e.g.*, 0.2 mol/L) is added to 6 mol/L KOH electrolyte to ensure the reversibility of the zinc electrochemical reactions [30,31].

2.2. Operation principles

The working principle of rechargeable zinc-air battery is that oxygen (the cathode) and metal zinc (the anode) undergo an electrochemical reaction in alkaline solution to recharge the battery. In other words, this process generates zinc oxide from elemental zinc and oxygen. In alkaline aqueous solution, the dissolution of the zinc electrode is divided into two steps. The first is the oxidation of zinc to zincate ($Zn(OH)_4^{2-}$). The zinc oxide then precipitates when it is dissolved and saturated during the discharge process [32]:

$$\text{Anode: } Zn + 4OH^- \rightarrow Zn(OH)_4^{2-} + 2e^- \quad (1)$$

$$Zn(OH)_4^{2-} \rightarrow ZnO + 2OH^- + H_2O \quad (2)$$

$$\text{Cathode: } O_2 + 2H_2O + 4e^- \rightarrow 4OH^- \quad (3)$$

$$\text{Overall: } 2Zn + O_2 \rightarrow 2ZnO \quad (4)$$

During the charging process, the reaction of the anode and cathode electrodes is completely reversible. The reduction reaction occurs in the zinc electrode. That is, $Zn(OH)_4^{2-}$ ions are reduced to elemental Zn. The air electrode provides an oxidation reaction to produce oxygen. Finally, ZnO decomposes into Zn and O_2.

Theoretically, the standard electromotive force of a zinc-air battery relative to a standard hydrogen electrode is 1.65 V. However, in actual operation, the actual discharge voltage is lower than 1.65 V due to the internal loss of the battery, resistance polarization, and concentration loss. The charging voltage must be higher than 1.65 V to complete the charging process and is decided by the current density and the performance of the air electrode catalyst. As discussed above, the discharging and charging processes correspond to the basic electrochemical reactions (ORR and OER) at the air cathode. The overpotential of the air cathode plays a key role in the charge and discharge voltage of the battery. In order to construct a rechargeable zinc-air battery with a high energy density and good cycle durability, the air (oxygen) electrode needs to have an efficient and stable bifunctional catalytic activity. This is because during both the charging and discharging processes, the overpotential of the electrode increases rapidly with enhancement of current density. Therefore, the development of an air electrode with highly efficient bifunctional catalytic performance is necessary to effectively promote the ORR and OER process.

2.3. Reaction mechanism for ORR and OER

OER and ORR are a pair of reversible reactions in electrochemical energy conversion equipment. They are the key to the future of zinc-air battery systems. However, slow dynamics and limited reversibility are the main obstacles that limit the efficiency of zinc-air battery [30,33]. The ORR mechanism is very complex, involving a large number of intermediate products. Currently, it is generally accepted that the reaction process in alkaline solution proceeds according to the direct four-electron pathway ($O_2 + 2H_2O + 4e^- \rightarrow 4OH^-$) or the two-electron pathway ($O_2 + H_2O + 2e^- \rightarrow HO_2^- + OH^-$, $HO_2^- + H_2O + 2e^- \rightarrow 3OH^-$) [34,35].

When ORR follows the two-electron pathway, a large number of intermediate products (HO_2^- or H_2O_2) are produced. This reduces the efficiency of the reaction and leads to corrosion and deactivation of the catalyst, affecting the energy conversion rate and long-term life of the battery. When ORR follows the four-electron pathway, O_2 is directly reduced to H_2O or OH^-, which avoids corrosion of the catalyst and improves the energy conversion rate and cycle life of the battery [36]. However, in practice, ORR is usually a mixed transfer reaction that includes both the two-electron and

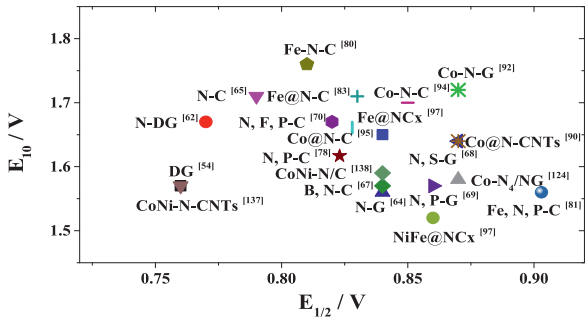

Fig. 2. Summary of electrocatalytic activity of recently reported bifunctional catalysts.

four-electron pathways. Therefore, finding a suitable catalyst to enhance the four-electron pathway is necessary for development of efficient zinc-air battery.

The mechanism of OER is different and more complex than that of ORR. A large number of intermediate products are produced during a multi-step electron transfer process [37–39]. Therefore, it is imperative to develop a catalyst that increases the OER reaction rate and reduces its activation energy.

3. Bifunctional oxygen electrocatalysts

At present, the precious metal-based catalysts Ru/IrO_2 and Pt/C demonstrate the best performance for OER and ORR, respectively. However, these catalysts are usually monofunctional. While a simple mixture of Ru/IrO_2 and Pt/C can be used as a bifunctional electrocatalyst, the complex preparation process, expensive material costs, and poor stability of precious metals significantly limit their development in zinc-air battery [40–42]. Therefore, the design and development of cheap and stable non-precious metal catalysts have become a research hotspot.

Carbon materials are an important catalyst for zinc-air battery, with the advantages of low cost, good stability, large specific surface, and high conductivity [43–46]. In addition, their electronic structures can be easily modified by defect engineering, heteroatom doping, or combination with other substances to improve electrocatalytic performance [47–49]. This paper will review the recent development of carbon-based materials as efficient and stable bifunctional electrocatalysts and outline future development directions.

The activities of different reported catalysts are displayed in detail in Fig. 2. The X-axis represents ORR activity at the half-wave potential ($E_{1/2}$). Catalysts with higher $E_{1/2}$ values have better performance. The Y-axis represents OER activity when the current density is 10 mA/cm^2 (E_{10}). Lower E_{10} values mean better performance. As can be seen, transition metal doping can significantly improve the activity of bifunctional electrocatalysts. The activity of these catalysts mainly depends on the unsaturated coordination bond in the active center or changes to the microstructure caused by the metal atoms. However, since most transition metal-based catalysts rely on surface reactions, some metal atoms in these catalysts cannot contact the reactants, resulting in low metal atom utilization. Therefore, reducing the geometric size of catalyst particles can improve electrocatalytic performance. The preparation of homogeneous monoatomic catalysts to improve the utilization rate of each metal atom and increase the proportion of low coordination metal centers should be the focus of future research.

3.1. Dopant-free carbon materials

The electrocatalytic process takes place on the surface of the electrocatalyst. Therefore, designing and controlling the surface of

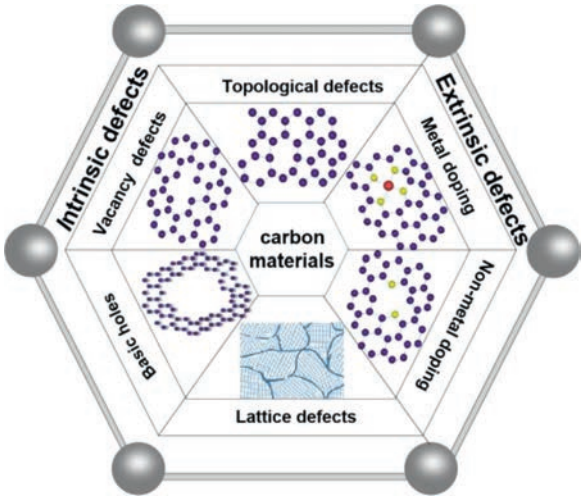

Fig. 3. Different carbon material defects.

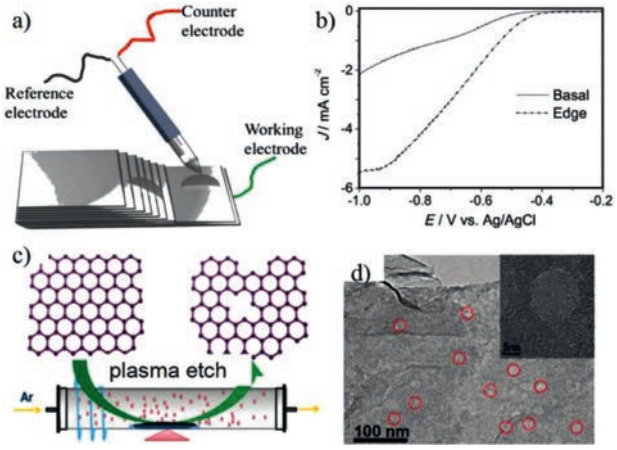

Fig. 4. (a) Schematic diagram of ORR test. (b) LSV curves of highly oriented pyrolytic graphite. Reprinted with permisison [53]. Copyright 2014, Wiley-VCH. (c) Schematic diagram of the synthesis of edge-rich graphene by Ar plasma etching. (d) TEM images of Ar plasma-treated graphene. Reprinted with permisison [57]. Copyright 2014, Wiley-VCH.

electrocatalysts is a key factor in catalyst design. In addition to the intrinsic characteristics of carbon materials, a large number of early studies have shown that the surface defects of electrocatalysts such as impurity defects, vacancy defects, and interstitial defects have a positive effect on electrocatalytic performance (Fig. 3) [50–52].

Recent reports on defective catalysts for oxygen electrodes are described below, as well as an analysis of how these defects affect electrocatalytic activity. Wang *et al.* used highly oriented pyrolytic graphite as an ORR catalyst and attempted to determine the active sites in the graphite [53]. A schematic diagram of the ORR test performed at the designated location is shown in Figs. 4a and b show that compared with the base plane, the edge has a higher onset potential and a larger current density. This is the first direct evidence that the edge of graphite is more active than the basal plane. To verify this hypothesis, they prepared graphite materials with more exposed edges by ball milling. Electrochemical tests confirmed that a higher number of exposed graphite edges results in better ORR electrocatalytic performance. At the same time, Hu *et al.* also showed that defective carbon materials can improve electrocatalytic activity [54], providing guidance for edge/defect engineering to improve catalytic activity.

With these findings, it is reasonable to claim that catalytic activity of the base surface of carbon materials is not as good as

catalytic activity of the edge. This provides a clear direction for the design of highly efficient carbon-based electrocatalysts to replace existing commercial catalysts. In-depth research has been conducted on the design of defective carbon-based electrocatalysts. Dai *et al.* reported that the use of quantum dots carried by graphene nanoribbons reduced the size of carbon materials, exposing more edges/defects and demonstrating good electrocatalytic performance [55]. Yao *et al.* used a simple denitrification procedure to remove nitrogen from N-doped graphene, creating various carbon defects [56]. Density functional theory (DFT) calculations revealed that the topological defects formed in the resulting bifunctional catalyst were the real active sites.

Carbon materials can be prepared at high temperatures or with a template method to form more defect structures. However, these methods cannot control the generation of edge defects. With an understanding of the positive effect of edge defects on catalytic activity, the development of new methods to prepare carbon-based materials with a large number of exposed edges is very important. Tao and co-workers reported the first use of a plasma etching method for the development of graphene with rich defects as an efficient electrocatalyst. The sample preparation diagram for this method is shown in Fig. 4c [57]. This plasma etching method can control the generation of edge defects and be used to prepare carbon materials with more exposed edges. Transmission electron microscope (TEM) images (Fig. 4d) clearly show that plasma treatment produces nano-sized holes but does not change the macroscopic structure of the graphene. This structure has an abundance of active sites and good conductivity. Electrochemical tests found that this material has significant electrocatalytic activity and good stability. Therefore, plasma technology is an effective method for controlling the formation of defects in carbon-based materials. This method shows significant promise for the treatment of other electrocatalysts in the future.

The research discussed in this section has successfully demonstrated the important role of defects in improving the electrochemical performance of carbon-based materials. Although these prepared catalysts cannot yet replace commercial catalysts, the combination of heteroatom doping and edge effects shows great potential for the further improvement of catalyst performance.

3.2. Heteroatom-doped carbon materials

Many studies have shown that heteroatom doping can increase the number of catalytic active sites on carbon materials and improve catalytic activity. These improvements are caused by changes to the internal structure of the carbon and to the electron density distribution of carbon atoms adjacent to the doped heteroatoms [58–61].

3.2.1. Mono-element doping

Although carbon materials have a high surface area and good conductivity, the oxygen reduction process of pure carbon materials is dominated by the two-electron pathway, resulting in poor ORR activity. By intentionally introducing N, B, O, S, P or other heteroatoms to the carbon structure, the four-electron pathway can be promoted, significantly improving the ORR activity of the doped carbon materials. Among these elements, nitrogen-doped carbon materials have been the most widely studied for use as efficient bifunctional oxygen catalysts. Zhang's team used a template method to prepare a defect-rich N-doped carbon material [62]. High resolution transmission electron microscopy (HRTEM) shows that the catalyst prepared by this method possesses a large number of pore structures. This catalyst exhibits good electrochemical activity with higher current density and a more negative onset potential (E_{onset}). By calculating the $E_{1/2}$ and E_{10}, the overall performance of the catalyst can be comprehensively judged. Fig. 5a shows that this catalyst has a small potential difference, demonstrating good potential for application in zinc-air battery. A zinc-air battery with this catalyst as the air cathode demonstrates a high open circuit voltage, good stability, and the ability to power a 2.2 V LED light. Theoretical calculations (Figs. 5b and c) show that the main reasons for improvement of catalyst performance are nitrogen doping, edge effects, and topological defects. These results have stimulated research on the reaction mechanism of catalysts and promoted the targeted design and manufacture of metal free carbon catalysts with defects for zinc-air battery.

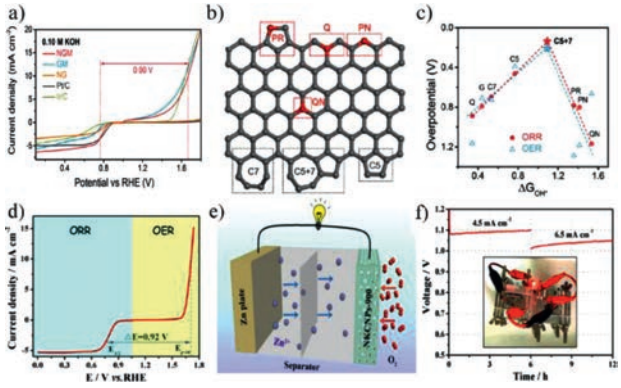

Fig. 5. (a) ORR/OER bifunctional activities of different catalysts. (b) Schematic diagram of graphene nanoribbon with various defects and N-doping (PR and PN represent pyrrolic nitrogen and pyridinic nitrogen, respectively; Q and QN represent quaternary nitrogen in the edge and bulk phase, respectively; C5 and C7 represent five-carbon and seven-carbon rings; C5+7 denotes a five-carbon ring adjacent to a seven-carbon ring). (c) ORR and OER volcano plots of overpotential *vs.* adsorption free energy of OH*. Reprinted with permisison [62]. Copyright 2014, Wiley-VCH. (d) Overall LSV plots of N-doped carbon nanoparticles catalysts. (e) Schematic diagram of basic zinc-air battery. (f) Constant current discharge curves (inset: photo of a red LED (≈ 3.0 V) powered by the catalyst). Reprinted with permisison [65]. Copyright 2018, American Chemical Society.

Nitrogen-substituted carbon materials include graphite nitrogen, pyridine nitrogen, and pyrrole nitrogen. Three forms with different proportions can be obtained by changing the nitrogen source, the temperature, and the synthesis method. Nevertheless, there is no definite conclusion about which form of nitrogen provides the largest enhancement to catalytic activity [63]. Yang *et al.* prepared a highly reactive nitrogen-doped graphene catalyst by controlling the carbonization temperature [64]. The zinc-air battery assembled with this catalyst has a high peak power density and specific capacity. It also demonstrates good cycle stability, and it was shown that the pyridine nitrogen structure plays the main catalytic role. Therefore, it can be concluded that the electrochemical performance of a catalyst is based on the effective design of catalyst structure. In turn, this is based on the introduction of defects and heteroatoms or adjustment of the geometric structure to increase the number of active sites and accelerate electron transfer. Wang *et al.* used a simple method to synthesize an excellent carbon material with a 3D structure rich in edge defects [65]. The unique three-dimensional structure of the catalyst accelerates the rapid mass transfer process, which is considered to be one of the reasons for its excellent activity (Fig. 5d). In addition, N doping in this carbon material leads to an increase in pyridine-N and graphite-N content, generating a large number of defects. It is known that N-doped edge defects redistribute charges and generate a charge difference, further enhancing electrochemical activity. Furthermore, a primary zinc-air battery assembled with this catalyst exhibits a high energy density and remarkable cycling stability (Figs. 5e and f). This bifunctional carbon-based electrocatalyst with a low cost, simple synthesis method, and metal-free composition

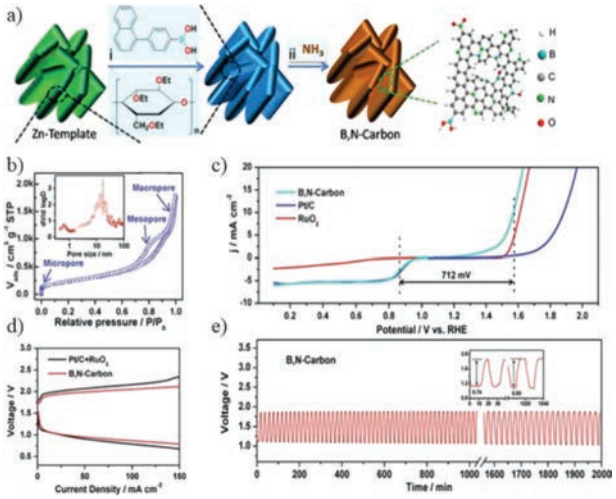

Fig. 6. (a) Schematic diagram of B,N-codoped carbon. (b) N_2 adsorption/desorption isotherm (inset: pore size distribution curve). (c) Overall LSV curve of catalysts. (d,e) Zn-air battery performance. Reprinted with permisison [67]. Copyright 2018, Wiley-VCH.

demonstrates excellent performance and great potential for zinc-air battery applications.

In order to create more defects and increase the content of pyridine nitrogen, Yi *et al.* used a $KMnO_4$ etching method to prepare a nitrogen-doped carbon catalyst [66]. The optimized material possesses a large number of defects and high level of pyridine-N content. It displays a significantly improved electrocatalytic activity and has the potential to replace commercial catalysts. In a zinc-air battery test, this nitrogen-doped carbon catalyst used as the air electrode demonstrated a similar energy density as Pt/C. To further explore the reaction mechanism, DFT calculations were performed to find that the active site is the second carbon close to pyridine-N.

Overall, these results conclusively demonstrate that introducing heteroatoms to create more defects in carbon structures is one of the most important methods for improving the electrocatalytic activity of metal-free carbon materials.

3.2.2. Multi-element doping

Dual-atom doping strategies can provide a synergistic effect to further improve the dual-function electrocatalytic activity of metal-free carbon materials. Sun *et al.* prepared a porous carbon nanomaterial codoped with B and N by a simple precipitation method (Fig. 6a) [67]. This material exhibits excellent bifunctional electrocatalytic activity due to the formation of rich defects and heteroatom doping. It can be inferred from Fig. 6b that the carbon material is rich in topological defects and edge defects. The hierarchical pore distribution is conducive to the diffusion of reactants and exposes more active sites. The difference in potential (ΔE) is an important parameter in evaluating the bifunctional catalytic activity of a catalyst ($\Delta E = E_{10}$ (OER) - $E_{1/2}$ (ORR)). Smaller ΔE values mean better electrocatalytic activity. As shown in Fig. 6c, the prepared B,N-doped catalyst has a lower ΔE value compared with other non-noble metal catalysts reported in recent literature ($\Delta E_{\text{B,N-codoped carbon}} = 0.712$ V; $\Delta E_{\text{N-doped carbon}} = 0.90$ V [62]; $\Delta E_{\text{S,N-codoped carbon}} = 0.77$ V [68]; $\Delta E_{\text{P,N-codoped graphene/carbon}} = 0.71$ V [69]). This B,N-doped catalyst even had a lower ΔE value than commercial catalysts. Furthermore, the assembled primary zinc-air battery exhibits high cell efficiency and good long-term stability (Figs. 6d and e).

Multi-doped carbon materials have also been widely studied due to their potential synergistic effect. Wu *et al.* explored the influence of ternary doped materials as bifunctional catalysts. They successfully synthesized a N,F,P-codoped homogeneous carbon catalyst by electrospinning method [70], finding that the obtained porous 3D network structure accelerated the mass transfer process and increased the specific surface area. Furthermore, the doping of heteroatoms induced charge distribution. This catalyst exhibits good bifunctional catalytic activity. When assembled into batteries for testing, it shows great potential for primary zinc-air battery and rechargeable zinc-air battery applications.

Although it has been shown that the doping of heteroatoms (B, F, P, S and N) into carbon materials can enhance catalytic activity, these doped catalysts have poor stability in harsh environments. Combining heteroatom-doped carbon materials with transition metals can solve this problem to a certain extent while also generating new active sites to further improve catalytic activity [71,72].

3.3. Metallic doping of carbon materials

Transition metals have high ORR and OER catalytic activity but poor oxidation resistance. However, studies have been reported showing that composites of transition metals and nitrogen-doped carbon materials as ORR and OER bifunctional catalysts exhibit strong catalytic performance [73,74]. To date, the nature of metal/nitrogen/carbon (M/N/C) active sites is still controversial. Some scholars believe that the active sites are the chemical bonds formed by nitrogen and transition metals. Others suggest that transition metals are not active sites, but that they promote the formation of N/C active sites at high temperatures. Although there is not yet good agreement on the nature of these active sites, related studies have shown that differences in the reaction conditions (nitrogen source, metal type and content, carbon support, carbonization temperature, and carbonization time) have a significant impact on catalytic activity [75–79].

3.3.1. Metal nanoparticles

Fe-N/C was the first M/N/C material to attract the attention of researchers in the field of zinc-air battery due to its excellent bifunctional catalytic performance. During the ORR/OER process, the inner metal centers of Fe-N/C are protected from corrosion by the alkaline solution and oxidative conditions, which is conducive to good durability [80–82]. Wang *et al.* successfully synthesized high-density iron nanoparticles encapsulated in N-doped carbon nanoshells [83]. This mesoporous catalyst has a relatively large specific surface area and pore volume, promoting the exposure of active sites during the electrochemical reaction. A catalyst prepared at 700 °C has a smaller ΔE value, indicating that it has better electrochemical performance. After being assembled into a zinc-air battery, a maximum peak power density of 220 mW/cm^2 was reached at 0.72 V. This battery also demonstrates better charge-discharge performance and cycle durability compared with batteries based on Pt/C and IrO_2 catalysts. These results show that changing the iron precursor and the pyrolysis temperature can modify the nitrogen doping content and the surface area of the iron nanoparticles, allowing the design of an oxygen electrocatalyst with high catalytic activity and stability. In future research, further precise optimization of the structure and active sites of the catalyst may improve its performance.

Park *et al.* prepared a novel Fe-N/C material by carbonizing filamentous materials containing carbon powder and an iron source at high temperatures for flexible rechargeable zinc-air battery applications. The battery assembled with this catalyst exhibits a higher power density [84].

In addition to Fe-N/C, other M-N/C materials such as Co-N/C have been reported in recent years [85–87]. The electrochemical performance of these catalysts can be further optimized by fine

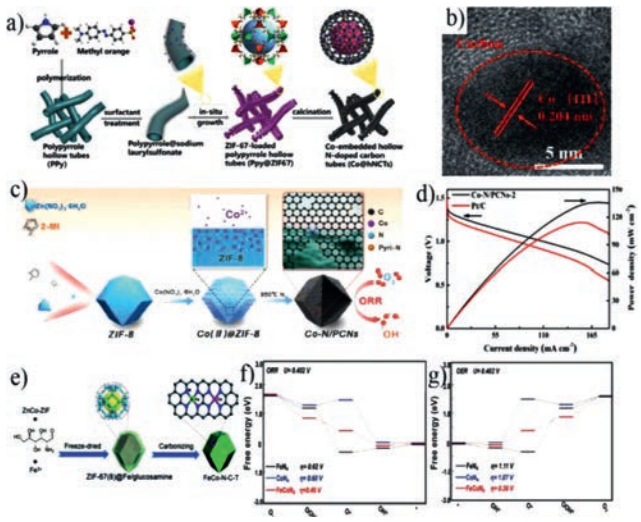

Fig. 7. (a) Illustration of the synthetic process for Co@N–CNTs catalysts. (b) HR-TEM image of Co@N–CNTs catalyst. Reprinted with permisison [90]. Copyright 2020, Elsevier Ltd. (c) Schematic diagram of Co-N/C catalyst synthesis. (d) Polarization and power density curves of Co-N/C and Pt/C catalysts. Reprinted with permisison [96]. Copyright 2020, Elsevier Ltd. (e) Schematic illustration of the synthesis of FeCo-N/-C catalysts. Free energy diagrams of (f) ORR and (g) OER processes on FeN_4, CoN_4 and $FeCoN_4$. Reprinted with permission [89]. Copyright 2020, Royal Society of Chemistry.

control of their morphology and microstructure. CNTs have hollow interiors and unique interwoven and macroporous properties which can significantly promote rapid electron transfer and the absorption of intermediates. Li *et al.* reported a Co,N-codoped carbon nanotube catalyst with excellent electrochemical performance which was constructed using a solution phase method [88]. Based on the unique winding structure inside the nanotubes and the synergistic effect of N and Co, rapid electron transfer is significantly enhanced. This is one of the major reasons for its excellent catalytic activity. A zinc-air battery assembled with the prepared catalyst exhibited high specific capacity (675.8 mAh/g) and high peak power density (159.83 mW/cm^2 at 0.63 V). At the same time, it also showed excellent cycle stability, with only a slight drop in voltage after 150 h of charge-discharge cycles.

Many studies have reported that metal organic frameworks (MOFs), which are three-dimensional porous materials with high specific surface area, high crystallinity, rich functional groups, and good structural stability, can simultaneously provide a carbon source, nitrogen source, and metal source for the synthesis of carbon-based catalysts. Therefore, MOFs are a hot material in the field of electrocatalysis [89-93]. Among these materials, research on zeolite imidazolate frameworks (ZIFs) has been increasingly reported in recent years. For instance, Gadipelli *et al.* developed a simple and facile way to synthesize a high-performance Co-N/C bifunctional electrocatalyst by using ZIFs as a precursor [94]. Zhang *et al.* successfully embedded Co particles into nitrogen-doped CNTs by pyrolysis of dicyandiamide and ZIF-67 [95]. Zhou *et al.* used a novel tube template orientation method to grow ZIF-67 *in situ* on the surface of polypyrrole nanometers and prepare Co and N codoped carbon nanotubes as a bifunctional catalyst (Fig. 7a) [90]. It can be clearly observed from Fig. 7b that the crystal lattice of 0.204 nm, which is attributed to the d space of Co (111) plane. This catalyst has high activity, high stability, and a power density of up to 149 mW/cm^2 in a zinc-air battery. After an aging test of 5000 cycles, its half-wave potential only decreases by 7 mV, demonstrating good cycle stability.

The existence of defects can be used to significantly improve catalytic activity. Therefore, accurate control of the morphology and structure of catalysts is the key to future research. Zhu *et al.* prepared Co-N/C nanomaterials by pyrolysis of Co ions encapsulated in ZIFs. These nanomaterials exhibit excellent electrochemical activity (Fig. 7c) [96]. In addition, it can be clearly observed that there is a high concentration of defects in the edges of the disordered graphite carbon after pyrolysis, revealing more active sites. The addition of Co ions produces a hollow structure, which increases the specific surface area. The performance of a zinc-air battery was tested with these Co, N-codoped carbon materials catalysts as the cathode. The maximum power density reached 135 mW/cm^2 (Fig. 7d). Almost no voltage loss was seen when the battery was discharged at 20 mA/cm^2 for 7 h, indicating that the battery has good cycle durability. The unique defects and rich hollow structure of this catalyst expose a large number of active sites, increase the surface area, and accelerate mass transfer, significantly enhancing catalytic activity. This explanation was confirmed by DFT calculations.

Compared with monometallic M/N/C composite materials, a synergistic effect can be achieved by using bimetallic materials to effectively improve the catalytic performance for ORR/OER. Through further modification, the intrinsic electronic and surface structure of the host material can also be manipulated. For this purpose, Zhu *et al.* calcined a MOF-based FeNi compound with melamine to prepare NiFe@N codoped graphene catalysts with a layered structure. These catalysts display excellent ORR and OER activity [97]. A zinc-air battery assembled with these catalysts is comparable to a commercial catalyst. However, while MOF-type materials have many advantages, they inevitably agglomerate during the pyrolysis process. Therefore, Duan *et al.* used glucosamine to encapsulate ZnCo-ZIF, followed by pyrolysis at 700 °C to successfully synthesize FeCo-N/C catalysts (Fig. 7e) [89]. In this MOF, Zn is very volatile at high temperatures, which improves the spatial dispersion of residual metals in the N–C matrix and significantly affects the composition and local nanostructure of the catalyst. The prepared catalysts have excellent bifunctional electrocatalytic activity. When used as an air cathode for a solid and liquid zinc-air battery, high peak power density and good cycle stability were achieved. The performance of this catalyst is better than that of commercial Pt/C + RuO_2. DFT calculations show that $FeCoN_8$ is more active than $FeCoN_4$, indicating that the synergistic effect of Co and Fe active sites can further improve electrocatalytic performance (Figs. 7f and g).

It is worth mentioning that metal-coordinated porphyrin molecules have been widely studied as cathode catalysts for zinc-air battery in recent years. These materials have many advantages, such as a stable coordination environment. Porphyrin ligands have redox activity, which promotes the multi-electron process. Furthermore, metal-coordinated porphyrins have a diverse range of structures [98–100]. However, their applications are limited due to their low electron transfer efficiency. Thus, for their application in zinc-air battery, the combination of these molecular catalysts with MOFs and other materials has been explored [101]. Loh and coworkers prepared a porphyrin-based MOF with Fe^{3+} as the node, significantly accelerating the electron transfer process [102]. Similarly, Liang *et al.* prepared MOF-supported Co porphyrins as a catalyst for oxygen electrocatalysis. When assembled into a zinc-air battery, it showed the same performance as a platinum-based material [103].

3.3.2. Single-atom catalysts

In order to reduce catalyst costs, reducing the size of metal nanoparticles to increase atom efficiency is an effective method that can also significantly enhance catalytic performance [104]. The atom is the smallest particle that maintains the chemical properties of an element. Single-atom catalysts (SACs) have attracted a growing amount of interest. This is due to their unique unsatu-

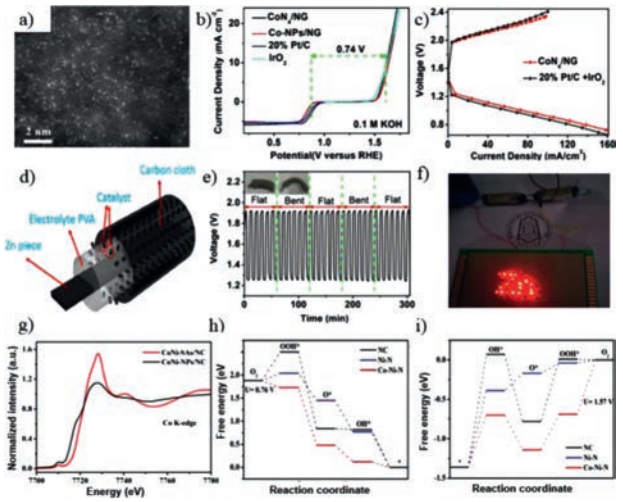

Fig. 8. (a) HAADF STEM image of CoN_4/NG catalyst. (b) Overpotential curves for different catalysts. (c-f) Performance of Zn-air battery with CoN_4/NG catalyst as the air electrode. Reprinted with permission [124]. Copyright 2018, Elsevier Ltd. (g) Co K-edge XANES spectra of CoNi/NC catalysts. Free energy diagrams of (h) ORR and (i) OER processes on NC, Ni-N and Co-Ni-N. Reprinted with permission [128]. Copyright 2020, Wiley-VCH.

rated coordination structure, the quantum size effect, and strong atom-supported interactions which can induce stable monatomic active sites in electrocatalysts [105–110]. However, due to the easy generation of nanoclusters or nanoparticles (NPs) through agglomeration, the design of SACs with dense dispersion is still a significant challenge. Therefore, the rational design of novel SACs with high activity, good selectivity, and good stability has attracted widespread attention. Researchers have focused on studying the structure-activity relationship of these catalysts at the atomic and molecular scales.

Reported SACs synthesis methods include mass-selected soft-landing, atomic layer deposition, coprecipitation, impregnation, MOF template, strong electrostatic, and photoreduction. Among these, the MOF template method has a significant advantage in the preparation of SACs due to its accurate control of the number of metal atoms and the structure of anchored complexes [111–119]. Since MOF-5 was used to synthesize porous carbon in 2008, many examples of manufactured MOF-derived nanomaterials have been reported [120–122]. For example, during the growth of ZIF-8, a monoatomic catalyst with excellent electrocatalytic performance, denoted Fe-Nx-C, was successfully synthesized by Han *et al.* [123]. A zinc-air battery assembled with this material demonstrated a long cycle life.

Yang *et al.* successfully applied SACs to foldable solid zinc-air battery using a surfactant-assisted method [124]. They prepared CoN_4/N codoped graphitic catalysts by doping Co ions into the g-C_3N_4 interlayer, finding that the atom-dispersed Co-N_x is a highly efficient catalytic active site. High-angle annular dark field scanning transmission electron microscopy (HAADF STEM) (Fig. 8a) was used to show that Co is evenly distributed on the graphite sheet. The overpotential curves diagrams of CoN_4/N codoped graphitic carbon and Co-NPs/N codoped graphitic carbon (Fig. 8b) show that the catalyst composed of single Co atoms has better catalytic activity ($\Delta E = 0.74$ V) than the catalyst composed of Co nanoparticles. In addition to traditional three-electrode electrochemical research, it has been reported that the application of CoN_4/N codoped graphitic carbon as an air cathode catalyst also shows good performance in rechargeable liquid zinc-air battery and foldable solid zinc-air battery. The energy density of these batteries is high and they have a long service life (Figs. 8c–f). These results are very promising for the application of single-atom catalysts in wearable flexible batteries, providing new ideas for the application of single-atom catalysts.

During the synthesis of SACs, heteroatoms (S, P and B) can be introduced into the carbon matrix and partial nitrogen atoms in the active sites of M-Nx can be replaced. The introduction of these heteroatoms breaks the electronic structure of the conventional active sites and can effectively enhance the electrocatalytic performance of SACs [125]. For example, S and N doping causes uneven charge distribution in the carbon skeleton, leading to positively charged carbon atoms. This is beneficial for the adsorption of oxygen. P doping helps shrink the adsorption of *OH intermediates and changes the electronic structure of the metal center, endowing the catalyst with bifunctional activity and improving ORR/OER activity [126]. Chen *et al.* prepared an electrocatalyst codoped with single iron atoms, nitrogen, sulfur, and phosphorus [127]. Long-distance phosphorus and sulfur interactions and close coordination of the nitrogen and metal framework were used to achieve electronic modulation of the active center. The synthesized catalyst has excellent performance, and its hollow form accelerates the slow kinetics. In addition, it also has great potential in H_2-air and zinc-air fuel cells.

While SACs have shown good application prospects in recent years and has shown many remarkable achievements in the field of zinc-air battery, their further application still faces huge challenges. There are two main reasons for this. One, the relationship between the linear ratio of reaction intermediates and the adsorption energy is difficult to determine because it depends on the single-atom active sites of SACs. This leads to a fundamental limitation of catalytic efficiency [128–130]. On the other hand, in order to avoid the aggregation of single metal atoms to form nanoparticles, the amount of metal supported on the catalyst has to be relatively low, resulting in a lower overall activity [131–134].

The introduction of dual atom catalysts (DACs) as a further extension of the SACs family of materials can further enhance catalytic activity [135,136]. The synergistic effect of the two metal atoms in DACs significantly improves the activity of these catalysts. The design of DACs provides new ideas for accurately controlling active sites at the atomic level and the rational design of bifunctional catalysts with multiple active sites and excellent performance. Inspired by this idea, Han *et al.* prepared heteroatom-doped dual-metal single-atom catalysts by pyrolysis of dopamine-coated metal-organic frameworks [137]. Due to the formation of a porous structure and the synergistic effect of the diatomic structure in the conductive carbon framework, the Co-Ni dispersed in the N-doped carbon materials has excellent bifunctional catalytic activity ($\Delta E = 0.81$ V), and a zinc-air battery assembled with this catalyst has a charge-discharge efficiency and cycle life superior to similar materials and even to Pt/C and IrO_2 catalysts. Co K-edge X-ray absorption near edge structure (XANES) curves (Fig. 8g) show that the near edge absorption energy of SACs is high, which indicates that Co single atoms in SACs have a more positive charge. The structural advantage of bimetallic monoatomic catalysts is highlighted by DFT analysis (Figs. 8h and i). To optimize the electrocatalytic performance of DACs, Li *et al.* prepared a two-sided electrocatalyst with atomically dispersed Co/Ni dual sites by introducing ZIF-67 [138]. Through reasonable design and synthesis of the composition and structure of the catalyst, the resulting catalyst exhibits good oxygen reaction performance. Through DFT calculations, it was determined that the synergistic effect of the Co/Ni-N-C atomic bond and microstructure can improve both ORR and OER performance, laying a new foundation for the development of efficient dual-atom catalysts.

At present, DACs research is still in an early stage, but compared with SACs, DACs show significantly enhanced catalytic activity under the synergistic effect of a high loading of two different metal

Table 1
Summary of electrocatalytic activities of recently reported bifunctional catalysts in 0.1 mol/L KOH.

Catalyst	Active material	$E_{1/2}$ (V)	E_{10} (V)	ΔE (V)	Ref.
DG	2D graphene with defects	0.76	1.57	0.81	[54]
N-DG	N-doped graphene mesh with defects	0.77	1.67	0.90	[62]
N-G	N-doped graphene nanoribbons with 3D architecture	0.84	1.56	0.72	[64]
N-C	N-doped carbon nanoparticles with edge defects	0.79	1.71	0.92	[65]
B, N-C	B,N-doped carbon with rich defects	0.84	1.57	0.73	[67]
N, S-G	N,S-codoped graphitic sheets	0.87	1.64	0.77	[68]
N, P-G	N,P-doped carbon	0.86	1.57	0.71	[69]
N, F, P-C	N,F,P ternary doped macroporouscarbon tubes	0.82	1.67	0.85	[70]
N, P-C	N,P-codoped defective carbon nanosheets	0.823	1.617	0.79	[78]
Fe, N-C	Fe,N-codoped carbon materials	0.81	1.76	0.95	[80]
Fe, N, P-C	Fe,N,P-doped defective carbon nanosheets	0.903	1.56	0.66	[81]
Fe@N-C	Fe NPs embedded in N-doped carbon nanoshell	0.83	1.71	0.88	[83]
Co@N-CNTs	Co NPs embedded in nitrogen doped hollow carbon tubes	0.87	1.64	0.76	[90]
Co-N-G	Co,N-codoped graphene with 3D porous structure	0.87	1.72	0.85	[92]
Co-N-C	Nitrogen doped and cobalt embedded nanoporous carbons	0.85	1.7	0.85	[94]
Co@N-C	Co NPs and nitrogen doped in ananocomposite	0.828	1.661	0.83	[95]
Fe@NC_X	Carbon encapsulated Fe nanocrystrals	0.84	1.65	0.81	[97]
NiFe@NC_X	Carbon encapsulated $NiFe_2$ alloy nanocrystrals	0.86	1.52	0.66	[97]
Co-N_4/NG	CoN_4 moieties dispersed on nitrogen-doped graphitic nanosheet	0.87	1.58	0.71	[124]
CoNi-N-CNTs	Co-Ni sites embedded in N-doped hollow carbon nanotubes	0.76	1.57	0.81	[137]
CoNi-N/C	Co/Ni and N-codoped porous carbon	0.84	1.59	0.75	[138]

Table 2
Summary of the performance of carbon-based catalysts as air electrodes in zinc-air battery.

Catalyst	Battery performance			Ref.
	Electrolyte/catalyst mass (mg/cm^2)	Δ (charge−discharge) E, V@j (mA/cm^2)	Power density (mW/cm^2)/specific capacity (mAh/g)/durability, cycle numbers (h)@j, (mA/cm^2)	
N-G	6 mol/L KOH/0.8	–	3/–/(100 s)	[62]
N-G(3D)	6 mol/L KOH/0.5	1.09@20	65/873/(30 h)@20	[64]
N-C	6 mol/L KOH	0.92@10	131.4/–/575@10	[65]
N-CNT	6 mol/L KOH/0.15	–	122/714/–@10	[66]
B, N-C	6 mol/L KOH + 0.2 mol/L $Zn(OAc)_2$	0.74@5	143/–/(24 h)@5	[67]
Co,N-G	6 mol/L KOH/2	0.76@20	108/709/300@ 20	[75]
Fe, N-C	6 mol/L KOH + 0.2 mol/L $Zn(OAc)_2$/1.57	0.7@2	–/501.3/(10 h)@2	[80]
Fe, N, P-C	6 mol/L KOH + 0.2 mol/L $Zn(OAc)_2$/0.5	–	120/585/450(50 h)@5	[81]
Fe-N-C	6 mol/L KOH/2	–	55/638/100@10	[82]
Fe@N-C	6 mol/L KOH + 0.2 mol/L $Zn(OAc)_2$	0.7@10	220/–/100@10	[83]
Co/Co-N-C	6 mol/L KOH + 0.2 mol/L $Zn(OAc)_2$	0.82@10	132/–/1000@10	[85]
Co@NCNT	6 mol/L KOH + 0.2 mol/L $Zn(Ac)_2$	–	159.83/675.8/300(150 h)@5	[88]
Fe,Co@N-C	6 mol/L KOH + 0.2 mol/L $Zn(OAc)_2$/3	0.9@10	150/518/(60 h)@1	[89]
Co@N-CNTs	6 mol/L KOH + 0.2 mol/L $Zn(OAc)_2$	0.82@5	149/746/(500 h)@5	[90]
Co-N-C	6 mol/L KOH + 0.2 mol/L $Zn(OAc)_2$/5	–	102.3/–/(12 h)@20	[91]
Co-N-G(3D)	6 mol/L KOH + 0.2 mol/L $Zn(OAc)_2$/3	0.96@20	119/–/250@5	[92]
Co@N-C	6 mol/L KOH + 0.2 mol/L $Zn(OAc)_2$/1	–	138.82/–/(16 h)@10	[95]
NiFe@NC_X	6 mol/L KOH + 0.2 mol/L $Zn(OAc)_2$	0.78@50	85/583.7/200@10	[97]
Fe-Nx-C	6 mol/L KOH + 0.2 mol/L $Zn(OAc)_2$	0.891@10	96/641/500(250 h)@10	[123]
Co-N_4/NG	6 mol/L KOH + 0.2 mol/L ZnO/1	0.84@10	115/730/(100 h)@10	[124]
Fe/NPS-C	6 mol/L KOH + 0.2 mol/L $Zn(OAc)_2$/1	0.96@5	195/–/(5.5 h)@5	[127]
CoNi-N-CNTs	6.0 mol/L KOH + 0.2 mol/L $Zn(Ac)_2$	0.89@10	101.4/750.9/95@5	[137]

atoms. However, current DACs research mainly focuses on ORR and CO_2RR. This overview provides a guide for scholars to investigate DACs in future research.

In order to provide readers with a more detailed description of the latest progress in this field, we have summarized the electrocatalytic activities of representative materials reported in recent years, shown in Table 1. A summary of carbon-based catalysts as air electrodes in zinc-air battery is reported in Table 2. As can be seen, single-atom catalysts show the most potential as bifunctional oxygen electrocatalysts for the practical application of zinc-air battery.

4. Summary and outlook

Zinc-air battery have broad application prospects in renewable electricity storage and transformation, but their efficiency is seriously affected by poor ORR and OER activity. Therefore, the development of bifunctional oxygen catalysts with excellent electrocatalytic activity is required for their further development. At present, precious metal materials are the most effective catalysts for ORR/OER, but their high cost, poor bifunctional activity, and low stability greatly limit their development. Therefore, this review focuses on the recent research advances of carbon-based bifunctional oxygen catalysts including metal-free carbon materials and carbon-based transition metal materials as air cathodes for zinc-air battery. In general, single-atom catalysts are by far the most promising non-noble metal catalysts for zinc-air battery. By optimizing the size, morphology, and structure of these catalysts, we expect that their performance in zinc-air battery will soar to unprecedented heights. This review offers guidance for the design and synthesis of electrocatalysts. The future development of these carbon-based materials should focus on three main directions, shown in Fig. 9 and described below:

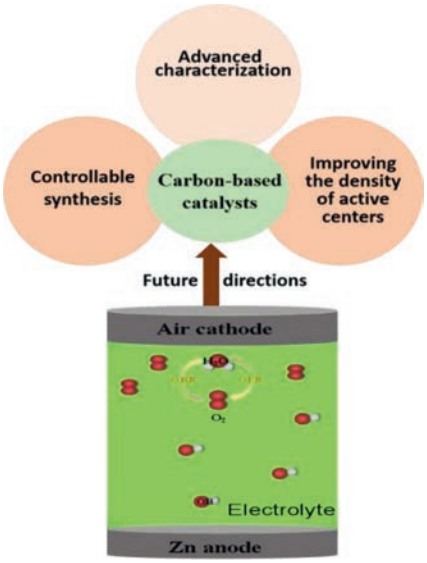

Fig. 9. Future development directions of carbon-based catalysts for zinc-air battery.

(1) Controlled synthesis of carbon-based materials. Currently, it has been shown that the existence of defects in electrocatalysts improves their performance, but it is very difficult to create desirable and effective defects in these carbon materials. The reasonable design and development of carbon-based porous materials (with precise control of the carbon micro/nanostructure) is a promising method for achieving good control of defects. Furthermore, the exploration of the synergistic effect of multiple components to combine the characteristics of different components and create active sites with a specific structure should be further explored. For metal/nitrogen/carbon catalysts, it is particularly important to control the structure evolution on the micro/nanoscale because most of these catalysts are prepared by high-temperature pyrolysis.

(2) Advanced characterization of carbon-based materials. Due to the restrictions of micro/nanoscale analysis, it is difficult to directly and accurately determine the mechanism of these catalysts, so the nature of their active sites is still controversial. From this point of view, future research should explore new experimental methods and use advanced *in situ* characterization techniques to identify the real active species and reveal the reaction process. This will be helpful for designing highly efficient electrocatalysts in practical applications.

(3) Improving the density of active centers in SACs. SACs can significantly improve catalyst activity, but due to the inevitable agglomeration of metal atoms during the synthesis process as well as the limitations of low metal loading, the preparation of highly dispersed SACs with high metal loading is still a key challenge. Although the development of DACs has led to an improvement in the density of active sites and catalytic performance due to the synergistic effect of different metal atoms, these dual atom sites are easier to aggregate or alloy. Furthermore, it is difficult to accurately determine the metal proportion in DACs, which limits the full utilization of the synergistic effect between different metal atoms. In addition, it is also difficult to accurately identify the active sites of DACs. Therefore, designing strong metal-support interactions and more effective synthesis strategies to avoid agglomeration will be necessary for further development of SACs and DACs.

In conclusion, these carbon-based materials require a significant amount of development before they will be able to replace precious metal catalysts in zinc-air battery. However, there is no doubt that single-atom catalysts will continue to be rapidly developed. It is expected that more efficient atomic electrocatalysts will be developed for zinc-air battery applications in the future.

Declaration of competing interest

The authors declare no conflict of interest.

Acknowledgements

We gratefully acknowledge the financial support from the National Natural Science Foundation of China (No. 21601076) and the Natural Science Foundation of Liaoning Province (No. 2019-ZD-0266).

References

[1] Y.Y. Huang, Y.Q. Wang, C. Tang, et al., Adv. Mater. 31 (2019) 1803800.
[2] X.B. Li, X.H. Gao, P.Y. Xu, et al., ACS Sustainable Chem. Eng. 7 (2019) 7148–7154.
[3] S.Z. Liu, W. Hall, B.C. Cui, et al., J. Power. Sources 342 (2017) 435–441.
[4] R. Du, Y.F. Wu, Y.C. Yang, et al., Adv. Energy Mater. 11 (2021) 2100154.
[5] J. Yu, C.X. Zhao, J.N. Liu, et al., Green Chem. Engin. 1 (2020) 117–123.
[6] J. Pan, Y.Y. Xu, H. Yang, et al., Adv. Sci. 5 (2018) 1700691–1700720.
[7] D.P. He, Y.L. Xiong, J.L. Yang, et al., J. Mater. Chem. A 5 (2017) 1930–1934.
[8] X.M. Liu, X.Y. Cui, K. Dastafkan, et al., J. Energy Chem. 53 (2021) 290–302.
[9] Y.Z. Li, R. Cao, L.B. Li, et al., Small 16 (2020) 1906735.
[10] M.C. Luo, Z.L. Zhao, Y.L. Zhang, et al., Nature 574 (2019) 81–85.
[11] X. Peng, T.J. Omasta, E. Magliocca, et al., Angew. Chem. Int. Ed. 58 (2019) 1046–1051.
[12] X.C. Chen, Z. Zhou, H.E. Karahan, et al., Small 14 (2018) 1801929.
[13] C. Tang, H.F. Wang, J.Q. Huang, et al., Electrochem. Energy Rev. 2 (2019) 332–371.
[14] S.C. Wang, Z.Y. Teng, C.Y. Wang, G.X. Wang, Chem. Sus. Chem. 11 (2018) 2267–2295.
[15] W. Li, R. Fang, Y. Xia, et al., Batteries Supercaps 2 (2019) 9–36.
[16] D. Song, W. Guo, T. Zhang, et al., Surf. Innov. 7 (2019) 10–17.
[17] J. Zhang, Q.X. Zhou, Y.W. Tang, L. Zhang, Y.G. Li, Chem. Sci. 10 (2019) 8924–8929.
[18] G.W. Heise, US Patent (1933) 1899615.
[19] J.H. Park, C.H. Lee, J.M. Ju, et al., Adv. Funct. Mater. 31 (2021) 2101727–2101736.
[20] F. Wang, O. Borodin, T. Gao, et al., Nat. Mater. 17 (2018) 543–549.
[21] R.J. Chen, R. Luo, Y.X. Huang, F. Wu, L. Li, Adv. Sci. 3 (2016) 1600051.
[22] T.P. Zhou, N. Zhang, C.Z. Wu, Y. Xie, Energy Environ. Sci. 13 (2020) 1132–1153.
[23] A. Radwan, H.H. Jin, B.S. Liu, et al., Carbon 171 (2021) 368–375.
[24] Y.J. Wang, B.Z. Fang, D. Zhang, et al., Electrochem. Energy Rev. 1 (2018) 1–34.
[25] X.X. Yu, T.P. Zhou, J.K. Ge, C.Z. Wu, ACS Mater. Lett. 2 (2020) 1423–1434.
[26] A.R. Mainar, O. Leonet, M. Bengoechea, et al., Int. J. Energy Res. 40 (2016) 1032–1049.
[27] Y.P. Deng, R.L. Liang, G.P. Jiang, et al., ACS Energy Lett. 5 (2020) 1665–1675.
[28] J.K. Wu, B. Liu, X.Y. Fan, et al., Carbon Energy 2 (2020) 1–17.
[29] J. Yi, X.Y. Liu, P.C. Liang, et al., Organomet. 38 (2019) 1186–1199.
[30] Y.P. Lei, Q.C. Wang, Z.Y. Chen, et al., J. Mater. Chem. A 6 (2018) 516–526.
[31] J. Pan, Y.Y. Xu, H. Yang, et al., Adv. Sci. 5 (2018) 1700691–1700720.
[32] Y.C. Wang, F.L. Chu, J. Zeng, et al., ACS Nano. 15 (2021) 210–239.
[33] B.Q. Li, S.Y. Zhang, B. Wang, et al., Energy Environ. Sci. 11 (2018) 1723–1729.
[34] Z.F. Huang, J. Wang, Y.C. Peng, et al., Adv. Energy. Mater. 7 (2017) 1700544.
[35] Y. Gao, Z.W. Cai, X.C. Wu, et al., ACS Catal. 8 (2018) 10364–10374.
[36] J.J. Wang, H. Hu, H. Zhang, et al., Energy Fuels 35 (2021) 6483–6503.
[37] J.W. Zhao, Z.X. Shi, C.F. Li, Q. Ren, G.R. Li, ACS Materials Lett. 3 (2021) 721–737.
[38] C. Beall, E. Fabbri, T. Schmidt, ACS Catal. 11 (2021) 3094–3114.
[39] C. Feng, M. Bilal Faheem, J. Fu, et al., ACS Catal. 10 (2020) 4019–4047.
[40] Z.K. Yang, Y. Wang, M.Z. Zhu, et al., ACS Catal. 9 (2019) 2158–2163.
[41] A. Majeed, P.X. Hou, F. Zhang, et al., Adv. Sci. 6 (2019) 1802177.
[42] H.M. Liu, X.N. Huang, Z.J. Lu, et al., Nanoscale 12 (2020) 9628–9639.
[43] S.Y. Wang, S.M. Chen, L.T. Ma, J.A. Zapien, Mater. Today Energy 20 (2021) 100659–100689.
[44] H.F. Wang, C. Tang, Q. Zhang, Catal. Today 301 (2017) 25–31.
[45] D. Yang, D. Chen, Y. Jiang, et al., Carbon Energy 3 (2021) 50–65.
[46] J.K. Wu, B. Liu, X.Y. Fan, et al., Carbon Energy 2 (2020) 370–386.
[47] H. Wang, Y. Shao, S.L. Mei, et al., Chem. Rev. 120 (2020) 9363–9419.
[48] J.F. Sun, Q.Q. Xu, J.L. Qi, et al., ACS Sustainable Chem. Eng. 8 (2020) 14630–14656.
[49] H.R. Pan, X.N. Huang, Z.J. Lu, et al., Chem. Eng. J. 419 (2021) 129619.
[50] Q.L. Wu, Q. Liu, Y.J. Zhou, et al., ACS Appl. Mater. Inter. 10 (2018) 39735–39744.
[51] X.C. Yan, Y. Jia, X.D. Yao, Chem. Soc. Rev. 47 (2018) 7628–7658.
[52] D.F. Yan, Y.X. Li, J. Huo, et al., Adv. Mater. 29 (2017) 1606459.
[53] A. Shen, Y. Zou, Q. Wang, et al., Angew. Chem. Int. Ed. 53 (2014) 10804–10809.
[54] Y.F. Jiang, L.J. Yang, T. Sun, et al., ACS Catal. 5 (2015) 6707–6712.

[55] H. Jin, H.H. Huang, Y.H. He, et al., J. Am. Chem. Soc. 137 (2015) 7588–7591.
[56] Y. Jia, L. Zhang, A. Du, et al., Adv. Mater. 28 (2016) 9532–9538.
[57] L. Tao, Q. Wang, S. Dou, et al., Chem. Commun. 52 (2016) 2764–2767.
[58] Y.Q. Zhang, L. Guo, L. Tao, Y.B. Lu, S.Y. Wang, Small Methods 29 (2018) 1800406.
[59] H.M. Liu, J.X. Cheng, Z.J. Lu, et al., Electrochim. Acta 312 (2019) 22–30.
[60] J. Quílez-Bermejo, E. Morallón, D. Cazorla-Amorósa, Carbon 165 (2020) 434–454.
[61] C. Sathiskumar, S. Ramakrishnan, M. Vinothkannan, et al., Nanomaterials 10 (2020) 76–91.
[62] C. Tang, H.F. Wang, X. Chen, et al., Adv. Mater. 28 (2016) 6845–6851.
[63] J.T. Ren, G.G. Yuan, C.C. Weng, L. Chen, Z.Y. Yuan, Chem. Cat. Chem. 10 (2018) 5297–5305.
[64] H.B. Yang, J.W. Miao, S.F. Hung, et al., Sci. Adv. 2 (2016) 1501122.
[65] Q.C. Wang, Y.P. Lei, Y.G. Zhu, et al., ACS Appl. Mater. Inter. 10 (2018) 29448–29456.
[66] S.J. Yi, X.P. Qin, C.H. Liang, et al., Appl. Catal. B: Environ. 264 (2020) 118537–118574.
[67] T. Sun, J. Wang, C.T. Qiu, et al., Adv. Sci. 5 (2018) 1800036.
[68] C.G. Hu, L.M. Dai, Adv. Mater. 29 (2017) 1604942.
[69] R. Li, Z.D. Wei, X.L. Gou, ACS Catal. 5 (2015) 4133–4142.
[70] M.G. Wu, Y.Q. Wang, Z.X. Wei, et al., J. Mater. Chem. A 6 (2018) 10918–10925.
[71] L. Chen, L.L. Cui, Z.Z. Wang, et al., ACS Sustainable Chem. Eng. 8 (2020) 13147–13158.
[72] L.J. Yang, S.Z. Feng, G.C. Xu, B. Wei, L. Zhang, ACS Sustainable Chem. Eng. 7 (2019) 5462–5475.
[73] W.C. Jiang, Y.L. Li, Y.S. Xu, et al., Chem. Eng. J. 421 (2021) 129689.
[74] Z. Ma, K.X. Wang, Y.F. Qiu, et al., Energy 143 (2018) 43–55.
[75] J. Fu, F.M. Hassan, C. Zhong, et al., Adv. Mater. 29 (2017) 1702526.
[76] W.F. Xie, Z.H. Li, S. Jiang, et al., Chem. Eng. J. 373 (2019) 734–743.
[77] G. Anandhababu, S.C. Abbas, L. Jiangquan, et al., Dalton T. 46 (2017) 1803–1810.
[78] X.L. Tan, D.H. He, X.W. Zhang, J. Electrochem. 25 (2019) 601–607.
[79] T. Tang, W.J. Jiang, X.Z. Liu, et al., J. Am. Chem. Soc. 142 (2020) 7116–7127.
[80] J.-.S. Lee, S. Sarawutanukul, M. Sawangphruk, S. Horike, A.C.S. Sustain, Chem. Eng. 7 (2019) 4030–4036.
[81] W.Z. Cheng, P.F. Yuan, Z.R. Lv, et al., Appl. Catal. B: Environ. 260 (2020) 118198–118206.
[82] G.Y. Ren, L.L. Gao, C. Teng, et al., ACS Appl. Mater. Inter. 10 (2018) 10778–10785.
[83] J. Wang, H.H. Wu, D.F. Gao, et al., Nano Energy 13 (2015) 387–396.
[84] J. Park, M. Park, G. Nam, J. Lee, J. Cho, Adv. Mater. 27 (2015) 1396–1401.
[85] P. Yu, L. Wang, F.F. Sun, et al., Adv. Mater. 31 (2019) 1901666.
[86] W.F. Xie, Z.H. Li, S. Jiang, et al., Chem. Eng. J. 373 (2019) 734–743.
[87] J.Y. Qin, Z.W. Liu, D.Y. Wu, J. Yang, Appl. Catal. B: Environ. 278 (2020) 119300–119309.
[88] Y.P. Li, J.Y. Gao, F. Zhang, et al., J. Mater. Chem. A 6 (2018) 15523–15529.
[89] X.D. Duan, S.S. Ren, N. Pan, M.D. Zhang, H.G. Zheng, J. Mater. Chem. A 8 (2020) 9355–9363.
[90] Q.Y. Zhou, Z. Zhang, J. Cai, et al., Nano Energy 71 (2020) 104592–104601.
[91] J.C. Li, X.T. Wu, L.J. Chen, N. Li, Z.Q. Liu, Energy 156 (2018) 95–102.
[92] S.C. Cai, R. Wang, W. Yourey, et al., Sci. Bull. 64 (2019) 968–975.
[93] Y.J. Zhong, X.M. Xu, W. Wang, Z.P. Shao, Batteries Supercaps 2 (2019) 272–289.
[94] S. Gadipelli, T.T. Zhao, S. Shevlin, Z.X. Guo, Energy Environ. Sci. 9 (2016) 1661–1667.
[95] E.H. Zhang, Y. Xie, S.Q. Ci, et al., J. Mater. Chem. A 4 (2016) 17288–17298.
[96] Y. Zhu, Z.Y. Zhang, Z. Lei, et al., Carbon 167 (2020) 188–195.
[97] J.B. Zhu, M.L. Xiao, Y.L. Zhang, et al., ACS Catal. 6 (2016) 6335–6342.
[98] L.S. Xie, X.P. Zhang, B. Zhao, et al., Angew. Chem. Int. Ed. 60 (2021) 7576–7581.
[99] H.N. Qin, Y.Z. Wang, B. Wang, et al., J. Energy Chem. 53 (2021) 77–81.
[100] L.S. Xie, X.L. Li, B. Wang, et al., Angew. Chem. Int. Ed. 58 (2019) 18883–18887.
[101] Z.Z. Liang, H.Y. Wang, H.Q. Zheng, W. Zhang, R. Cao, Chem. Soc. Rev. 50 (2021) 2540–2581.
[102] M. Jahan, Q. Bao, K.P. Loh, J. Am. Chem. Soc. 134 (2012) 6707–6713.
[103] Z.Z. Liang, H.B. Guo, G.J. Zhou, et al., Angew. Chem. Int. Ed. 60 (2021) 8472–8476.
[104] Y. Peng, B.Z. Lu, S.W. Chen, Adv. Mater. 30 (2018) 1801995–1802072.
[105] Y.Q. Su, Y. Wang, J.X. Liu, et al., ACS Catal. 9 (2019) 3289–3297.
[106] X. Hai, X.X. Zhao, N. Guo, et al., ACS Catal. 10 (2020) 5862–5870.
[107] C. Du, Y.J. Gao, J.G. Wang, W. Chen, J. Mater. Chem. A 8 (2020) 9981–9990.
[108] B.Q. Li, C.X. Zhao, S.M. Chen, W. Chen, Adv. Mater. 31 (2019) 1900592.
[109] X.X. Wang, D. Cullen, Y.T. Pan, et al., Adv. Mater. 30 (2018) 1706758.
[110] S.L. Chou, Y. Wu, Q. Zhang, Y.M. Kang, Small Methods 3 (2019) 1900523–1900524.
[111] X. Liu, S.F. Jia, M. Yang, et al., Nat. Commun. 11 (2020) 4240–4247.
[112] K. Jiang, B.Y. Liu, M. Luo, et al., Nat. Commun. 10 (2019) 1743–1751.
[113] T. Gan, Y.F. Liu, Q. He, et al., ACS Sustainable Chem. Eng. 8 (2020) 8692–8699.
[114] D.X. Yan, J. Chen, H.P. Jia, Angew. Chem. Int. Ed. 59 (2020) 13562–13567.
[115] A.M. Abdel-Mageed, B. Rungtaweevoranit, M. Parlinska-Wojtan, et al., J. Am. Chem. Soc. 141 (2019) 5201–5210.
[116] Y. Zheng, S.Z. Qiao, Natl. Sci. Rev. 5 (2018) 626–627.
[117] Y.C. Wang, F.L. Chu, J. Zeng, et al., ACS Nano 15 (2021) 210–239.
[118] H.G. Huang, K. Shen, F.F. Chen, Y.W. Li, ACS Catal. 10 (2020) 6579–6607.
[119] A.J. Han, B.Q. Wang, A. Kumar, et al., Small Methods 3 (2019) 1800471.
[120] B. Liu, H. Shioyama, T. Akita, Q. Xu, J. Am. Chem. Soc. 130 (2008) 5390–5391.
[121] C.C. Hou, H.F. Wang, C.X. Li, Q. Xu, Energ. Environ. Sci. 13 (2020) 1658–1693.
[122] Y.S. Wei, M. Zhang, R.Q. Zou, Q. Xu, Chem. Rev. 120 (2020) 12089–12174.
[123] J.X. Han, X.Y. Meng, L. Lu, et al., Adv. Funct. Mater. 29 (2019) 1808872.
[124] L. Yang, L. Shi, D. Wang, Y.L. Lv, D.P. Cao, Nano Energy 50 (2018) 691–698.
[125] J.J. Guo, J.J. Huo, Y. Liu, et al., Small Methods 3 (2019) 1900159.
[126] Z.L. Jiang, W.M. Sun, H.S. Shang, et al., Energ. Environ. Sci. 12 (2019) 3508–3514.
[127] Y.J. Chen, S.F. Ji, S. Zhao, et al., Nat. Commun. 9 (2018) 5422–5433.
[128] Z.X. Song, L. Zhang, K. Doyle-Davis, et al., Adv. Energy Mater. 10 (2020) 2001561–2001602.
[129] J. Zhang, Q.A. Huang, J. Wang, et al., Chin. J. Catal. 41 (2020) 783–798.
[130] B.Z. Lu, Q.M. Liu, S.W. Chen, ACS Catal. 10 (2020) 7584–7618.
[131] X. Zhou, Q. Shen, K.D. Yuan, et al., J. Am. Chem. Soc. 140 (2018) 554–557.
[132] J. Li, S.G. Chen, N. Yang, et al., Angew. Chem. Inter. Ed. 58 (2019) 7035–7039.
[133] H.S. Shang, W.M. Sun, R. Sui, J.J. Pei, Y.D. Li, Nano Lett. 7 (2020) 5443–5450.
[134] S.R. Chen, M. Cui, Z.H. Yin, et al., ChemSusChem 14 (2021) 73–93.
[135] G.G. Yang, J.W. Zhu, P.F. Yuan, et al., Nat. Commun. 12 (2021) 1734–1743.
[136] Z.C. Yao, T. Tang, J.S. Hu, L.J. Wan, Energy Fuels 35 (2021) 6380–6401.
[137] X.P. Han, X.F. Ling, D.S. Yu, et al., Adv. Mater. 31 (2019) 1905622.
[138] Z.H. Li, H.Y. He, H.B. Cao, et al., Appl. Catal. B: Environ. 240 (2019) 112–121.